

Phase Coexistence Curves for Off-Lattice Polymer–Solvent Mixtures: Gibbs-Ensemble Simulations

John K. Brennan^{*,†} and William G. Madden[‡]

Department of Chemical Engineering and Materials Science, Wayne State University, Detroit, Michigan 48202

Received July 16, 2001; Revised Manuscript Received December 29, 2001

ABSTRACT: We present a simple and effective strategy for simulating the phase coexistence of off-lattice polymer–solvent mixtures when the solvent-rich phase contains negligible polymer. Under conditions sufficiently far from the solution critical point, an osmotic equilibrium is established between a pure solvent phase and a polymer-rich phase that produces a polymer-rich phase indistinguishable from the corresponding phase of the full binary mixture. Evaluation of the accuracy and reliability of the method is tested on a simple bead–spring model under both constant-pressure and constant-temperature conditions. A key advantage of the method over currently available techniques is that the insertion and deletion of chain molecules are not required. Though the method is illustrated for short, linear chains, it has even wider applicability for long, linear chains as well as for branched and networked chains. For many engineering applications, the method alone may suffice for simulating the relevant portion of the coexistence curve.

1. Introduction

The phase behavior of polymer–solvent systems has significant industrial implications.¹ From solvent casting to extractions to supercritical processing, solvents are often essential ingredients used in creating raw polymer and finished artifacts.^{2–16} Considerable theoretical effort has been expended on determining the properties of both dilute and concentrated polymer solutions. Historically, this focus has derived from the lattice theories introduced in the 1940s^{17–20} and from the early simulation efforts of lattice chains.^{21,22} A wide variety of theoretical models has been applied to polymer–solvent mixtures of industrial importance. Judging the origins of their successes and failures requires an accurate knowledge of the coexistence curves of the underlying microscopic models. It is only in the past decade that simulation results have become available for the coexistence curves of polymer blends and polymer–solvent systems.^{23–28} In the latter case, these have been largely confined to simulations within the lattice model and then only in the incompressible limit. This is unfortunate, since compressibility effects are crucial in giving rise to significant features of the coexistence curve, such as lower critical points. From the limited studies available, it has become clear that some of the older lattice theories have severe deficiencies and that several newer theories^{24,29,30} make significant improvements. Still, at higher temperatures, all the theories are significantly in error. (Interestingly, the theories seem to make better predictions for polymer–solvent systems than for polymer blends.^{23,24}) None of this was entirely unexpected, but the extent of the errors in the theories has finally been quantified—albeit only for lattice models.

Recently, several promising off-lattice theoretical approaches to bulk-phase polymer systems have been

introduced.^{31–43} Though most existing studies using these theories have focused on neat polymer and polymer blends, they can be generalized to polymer–solvent systems. However, the substantial conformational changes that are observed in polymer solutions pose a significant challenge that has yet to be addressed by any theory that attempts to span the full range of concentrations observed in experiment. In assessing the accuracy and reliability of these theories to predict phenomena involving phase equilibria, it will be essential to have suitable simulation data at hand. In addition, models that include a realistic level of atomic detail will probably be addressable only by simulation in the foreseeable future.

At about the same time that the polymer lattice studies were undertaken, revolutionary new methods for simulating the phase behavior of small molecule systems were introduced.^{45,46} The introduction of the Gibbs-ensemble method by Panagiotopoulos and co-workers^{47,48} greatly simplified the process of calculating coexistence curves by combining the search and evaluation processes into a single simulation. The Gibbs-ensemble method requires that a separate simulation cell be employed for each phase present. In its usual guise, the method requires that all species present be transferred from one of these cells to another using an insertion probability that enforces equality of chemical potential. The actual values of the chemical potentials need never be determined. In applying this technique to macromolecular systems, serious problems arise. The probability of accepting an overt insertion of long chains into dense media becomes improbably small as the molecular weight of the chain increases, even with the use of “smart insertion” techniques.^{49–54} Thus, the Gibbs-ensemble method has had only limited applicability to polymeric systems, generally involving the pure melt^{55–62} or polymer–solvent mixtures of short chains.²⁸

Several alternatives to the Gibbs-ensemble method have been introduced recently in attempts to seek remedies both for general phase equilibrium problems and for polymer-related problems. One such alternative

[†] Present address: Department of Chemical Engineering, North Carolina State University, Raleigh, NC 27695-7905.

[‡] Present address: Department of Natural Sciences, Lawrence Technological University, Southfield, MI 48075.

* Author of correspondence: e-mail jkbrennan@unity.ncsu.edu.

is a particle identity switch method, applied to small molecule mixtures by Kofke and Glandt⁶³ and to lattice polymer solutions by Sariban and Binder.²³ Another alternative method is the Gibbs–Duhem integration scheme recently introduced by Kofke^{64,65} for pure fluids which was later extended to mixtures by Mehta and Kofke.⁶⁶ The method is based on thermodynamic integration along a saturation line. For any given pair of points along the coexistence curve, the method is as straightforward as the Gibbs-ensemble scheme. However, unlike the Gibbs-ensemble method, many closely spaced points must be considered to ensure that the thermodynamic integration is accurate. In addition, a pair of coexisting points must be known a priori to initiate the integration procedure.

In this work, we present a method for simulating the phase coexistence of polymer–solvent mixtures using a variant of the conventional Gibbs-ensemble method—the osmotic Gibbs-ensemble. The method presented here relies on the well-founded assumption that at low temperatures the solvent-rich phase is essentially pure solvent. A key feature of the method is that it does not require the insertion or deletion of polymer chains. Although the method cannot be used to calculate the coexistence curve near the critical point, the portion of the phase diagram required for most engineering applications can be calculated. Furthermore, if the full coexistence curve is needed, the method can be combined with the Gibbs–Duhem integration scheme presented in previous work⁶⁷ to determine the complete phase diagram. The simulation strategy used in this work is presented in section 2, followed by an application of the method given in section 3. Finally, a brief discussion of the implications of the method is given in section 4.

2. Model and Method Strategy

For development purposes, we choose a simple model system consisting of a collection of n -bead chains immersed in a solution of single-site particles, with n varying from 10 to 100 beads. Solvent molecules and polymer beads that are not covalently bonded to one another interact through a standard Lennard-Jones potential

$$U_{\alpha\gamma}(r) = 4\epsilon_{\alpha\gamma} \left[\left(\frac{\sigma_{\alpha\gamma}}{r} \right)^{12} - \left(\frac{\sigma_{\alpha\gamma}}{r} \right)^6 \right] \quad (1)$$

where $\epsilon_{\alpha\gamma}$ and $\sigma_{\alpha\gamma}$ are suitable energy and size parameters for the species α and γ . The size parameters for the beads of the chain and for the solvent molecules are identical (i.e., $\sigma_{ss} = \sigma_{sp} = \sigma_{pp}$, where “s” indicates solvent and “p” indicates polymer). The energy parameters are also identical for beads of the same species (i.e., $\epsilon_{ss} = \epsilon_{pp}$), while the polymer–solvent bead interaction is $\epsilon_{sp} = 0.75\epsilon_{ss}$. This choice of ϵ_{sp} leads to a phase-separated system at low temperatures and/or low pressures while at high temperature or pressure the mixture is fully miscible. The interactions between the covalently bonded beads of the chain are represented by a moderately stiff harmonic spring:

$$U_b(r) = k_b(r - r_b)^2 \quad (2)$$

For this study, the equilibrium bond length, r_b , was set equal to σ_{ss} . The force constant was taken as $k_b =$

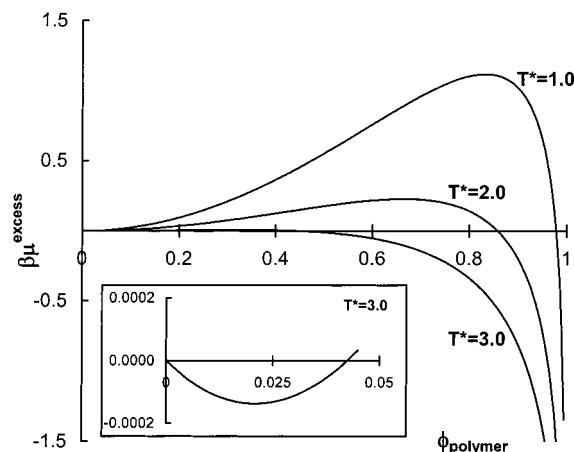


Figure 1. Excess solvent chemical potential as a function of polymer volume fraction as determined by the Flory–Huggins theory for chains of length 100 on a lattice with a coordination number of 6. $T^* = kT/\epsilon_{ss}$ and $\beta\mu^{\text{excess}} = \beta(\mu_s - \mu_s^0)$ where $\beta = 1/T^*$, μ_s is the solvent chemical potential in the mixture, and μ_s^0 is the pure solvent chemical potential.

$200\epsilon_{ss}\sigma_{ss}^{-2}$ which gives a root-mean-square variation of the bond length of about $0.1\sigma_{ss}$ for the temperatures and pressures under consideration here. These choices of r_b and k_b ensure well-developed chain character, while permitting fairly large Cartesian displacements of individual beads during the course of the simulations.

The strategy for simulating the phase equilibria of polymer–solvent systems proposed in this work relies first on the recognition that at low temperatures a polymer-rich solution is in equilibrium with a virtually pure solvent. Figure 1 illustrates this phenomenon using the Flory–Huggins theory to calculate the solvent chemical potential. The composition is described in terms of the particle site fractions ϕ_s and ϕ_p , where a “particle” is either a solvent molecule or an individual polymer bead. In Figure 1, the excess solvent chemical potential $\beta\mu_s^{\text{ex}} = \beta(\mu_s - \mu_s^0)$ is plotted as a function of ϕ_p , where μ_s^0 is the chemical potential of the pure solvent. For sufficiently low temperatures, $\beta\mu_s^{\text{ex}}$ is nearly flat for small ϕ_p , passing through a van der Waals loop as ϕ_p is increased and then plummeting rapidly at still higher concentrations. The initial negative departure from $\beta\mu_s^{\text{ex}} = 0$ cannot be discerned on the scale of the full figure and is illustrated in the inset for $T^* = kT/\epsilon_{ss} = 3.0$. As in any mean-field theory, the resulting curve shows “cubic” behavior. A spurious zero (also shown in the inset) is always found very close to the origin, especially for low temperatures and for long chain lengths.

Whatever the actual concentration of polymer in the solvent-rich phase, ϕ_p must be found in the very narrow domain where $\beta\mu_s^{\text{ex}} < 0$ and where the plot of $\beta\mu_s^{\text{ex}}$ vs ϕ_p has negative curvature. On the polymer-rich side, the curve drops so rapidly that any plausible value for $\beta\mu_s^{\text{ex}}$ in the solvent-rich phase maps onto an exquisitely small range of ϕ_p in the polymer-rich phase. Thus, the concentration in the polymer-rich phase is insensitive to small errors in choosing the correct solvent chemical potential. This issue was previously discussed by Madden et al.²⁴ in their report of the coexistence curve of lattice polymer–solvent systems. To establish the polymer-rich side of the coexistence curve at low temperatures, one need only determine the concentration at

which the solvent chemical potential is essentially equal to pure solvent at the same temperature and pressure. While the solvent remains exceedingly dilute, there is no need to consider the polymer chemical potential. (A very accurate equality of polymer chemical potentials is necessary to establish the precise value of ϕ_p —however small—on the solvent-rich side of the coexistence curve.)

The simple condition that a polymer-rich solution is in equilibrium with virtually pure solvent does not hold at higher temperatures. Consider the $T^* = 3.0$ curve of Figure 1, a temperature fairly close to the critical point for this model system in the context of the Flory–Huggins theory.¹⁷ The curve is now quite flat both near $\phi_p = 0$ and again when it recrosses the ϕ_p -axis at higher concentrations. At this temperature, the coexistence curve for the polymer-rich phase is not adequately determined by finding the condition $\beta\mu_s^{\text{ex}} = 0$. Calculating the composition of the coexisting phases then requires that the chemical potentials of both species be simultaneously matched. For the solvent, this will correspond to slightly negative values of $\beta\mu_s^{\text{ex}}$. The true coexistence curve will then be found to be shifted to discernibly higher concentrations than one would estimate from the condition $\beta\mu_s^{\text{ex}} = 0$. The point at which the more elaborate calculations are required roughly corresponds to the first significant presence of polymer in the solvent-rich phase.

The Flory–Huggins results shown in Figure 1 are interpreted as a binary solution in the incompressible (infinite pressure) limit. In real systems and in the bead–spring model employed here, the solutions are compressible, and pressure is a crucial variable. It is important to establish that the character of Figure 1 is valid for compressible systems under conditions that are not too near the critical point. Compressible lattice theories are plentiful, but molecular simulation can be more directly used to verify that the solvent chemical potential of our off-lattice model also exhibits the behavior shown in Figure 1. Therefore, we performed a series of isothermal–isobaric simulations for 20-bead chains immersed in a varying amount of solvent at $T^* = kT/\epsilon_{ss} = 1.8$ and $P^* = P\sigma_{ss}^3/\epsilon_{ss} = 1.0$. The solvent chemical potential was calculated by the standard Widom method of test particle insertions.⁶⁸ The dependence of the solvent chemical potential on the polymer number fraction ($\phi_p = \text{no. of monomer beads}/\text{total no. of beads}$) is shown in Figure 2. The off-lattice model exhibits similar behavior to that seen for the lattice model at $T^* = 1.0$ in Figure 1; i.e., μ_s is independent of ϕ_p at low concentrations while the curve drops precipitately at high ϕ_p . Therefore, the assumption that at low temperatures the solvent-rich phase is essentially pure is also valid for a compressible model solution.

Of course, for a macroscopic system only limited excursions into the metastable regions shown in Figure 2 would be possible. However, the choice of the ensemble (N_s, P, T), the relatively small size of the simulation cell (cell length $\approx 10\sigma_{ss}$), and the use of periodic boundary conditions suppress the fluctuations required for phase separation, leading to the cubic character also seen in Figure 1. For the low-temperature behavior shown in Figure 2, the initial negative departure of μ_s from its pure-solvent value is not observed. Nor is the recrossing of the axis observed because both of these behaviors occur at exceedingly small concentrations. However, only the behavior near $\beta\mu_s^{\text{ex}} = 0$ (at both high and low

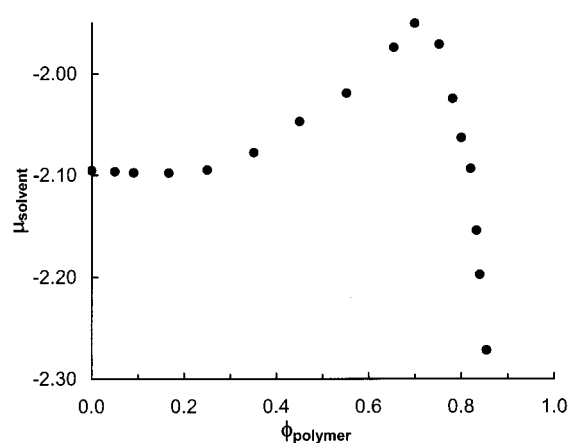


Figure 2. Solvent chemical potential in the presence of 20-bead chains for the off-lattice model described in the text at $T^* = 1.8$ and $P^* = 1.0$. Chemical potentials were determined via Widom insertion in an isothermal–isobaric ensemble simulation. The polymer mole fraction is defined as $\phi_{\text{polymer}} = \text{no. of monomer beads}/\text{total no. of beads}$.

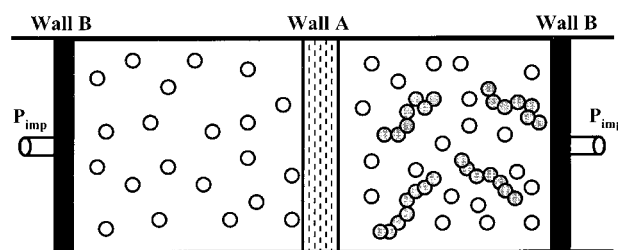


Figure 3. Schematic of the osmotic Gibbs-ensemble method used in this work for simulating polymer–solvent phase coexistence. Wall A is fixed and permeable to solvent molecules *only*. Wall B represents a movable piston that maintains the imposed pressure, P_{imposed} . Wall B is impermeable to both solvent and polymer molecules. The simulation cell to the reader's left represents the pure solvent phase, while the simulation cell to the reader's right represents the polymer-rich phase. White spheres represent solvent particles while gray spheres make up the polymer chains. This schematic is for illustration purposes only and not intended to represent the actual simulation setup.

ϕ_p) is relevant to the actual calculations of the methodology presented in this paper.

The condition $\beta\mu_s^{\text{ex}} = 0$ can be readily created from a Gibbs-ensemble simulation by implementing the following scheme. One of the simulation cells contains pure solvent, and the other cell contains polymer and solvent at polymer-rich conditions. Only solvent molecules are transferred between the simulation cells. In applying this restriction, we have (in effect) placed a semipermeable membrane between the phases. The result of this is a system at osmotic equilibrium. A schematic of the constant-pressure version of the osmotic Gibbs-ensemble simulation method is shown in Figure 3. In Figure 3, wall A represents a fixed boundary that only allows solvent molecules to be exchanged between the coexisting phases. The two wall B's are not fixed in space and represent pistons that maintain a selected pressure on the simulation cells. Note that Figure 3 is intended for illustration purposes only, and the actual simulation setup does not contain phase boundaries or rigid walls.

The true binary equilibrium (with polymer present in both simulation cells) differs only imperceptibly in composition from that established in the osmotic simu-

lation. This condition holds true while the solvent chemical potential has the character evinced in Figure 2. One normally thinks of this sort of equilibria as requiring the imposition of an additional pressure (i.e., the osmotic pressure) to establish equality of solvent chemical potential. An osmotic pressure would be needed if one attempted to place a highly dilute polymer solution in contact with pure solvent across a semipermeable membrane. In the absence of any pressure difference, the pure solvent would become exhausted of all molecules as the polymer-containing phase attempts to dilute itself to negligible concentration. However, Figure 2 shows that there is nothing preventing the more concentrated polymer solution from establishing a true equilibrium with the pure solvent across a membrane at the same temperature and pressure.

The Gibbs-ensemble method as described here is applicable for a significant fraction of the coexistence envelope. For very long chains or networked and branched chain systems, this may span the entire range of available experimental data and practical engineering interest.^{13–15} The longer the chains are, the broader the temperature range for which this strategy holds. Interestingly, for chains of infinite length (a limiting bound often considered in theoretical models), polymer can never cross from one phase to the other. Therefore, the “solvent-rich” side of the coexistence curve is always pure solvent, and $\beta\mu_s^{\text{ex}} = 0$ is the exact criteria for phase equilibrium at all temperatures. The method presented here satisfies these conditions and could serve as a valuable guide to uncovering deficiencies in theoretical models.

As the system temperature approaches the critical temperature of the solution and both phases begin to contain significant amounts of polymer, it becomes necessary to abandon the Gibbs-ensemble method described here and invoke some other phase coexistence method. Previously, Brennan has shown how results such as those obtained in the present paper can be used to initiate Gibbs–Duhem integration simulations at these higher temperatures.⁶⁷

3. Gibbs-Ensemble Simulations

The Gibbs-ensemble methodology for mixtures of small molecule systems has been thoroughly described elsewhere,^{45–48} and only a brief summary is presented here. A Gibbs-ensemble simulation requires two simulation cells that correspond to the macroscopic coexisting phases assumed to be far from the interface of the phase boundary. The simulation technique as employed here involves up to three distinct types of trial moves: particle displacements, solvent particle interchanges between the two cells, and volume rearrangements of the cells.

The Gibbs-ensemble simulations reported in this work, termed the osmotic Gibbs-ensemble method, are performed at constant pressure. (An analogous constant-volume version is also possible.) A solvent-only phase and a polymer-rich phase are simulated. Under these conditions, the total system (both cells taken together) explores an isothermal–isobaric ensemble where volume changes of the two cells (labeled I and II) occur independently. Particle displacements and solvent particle exchanges between the coexisting phases are carried out using the standard acceptance criteria.⁴⁸ An attempted volume change (which maintains the imposed

pressure, P) is accepted with a probability given by $\min(1, P_{\text{vol}})$, where P_{vol} is

$$P_{\text{vol}} = \exp \left(-\beta \left[\Delta E^{\text{I}} + \Delta E^{\text{II}} - N^{\text{I}} kT \ln \frac{V^{\text{I}} + \Delta V^{\text{I}}}{V^{\text{I}}} - N^{\text{II}} kT \ln \frac{V^{\text{II}} + \Delta V^{\text{II}}}{V^{\text{II}}} + P(\Delta V^{\text{I}} + \Delta V^{\text{II}}) \right] \right) \quad (3)$$

Typically, to achieve higher acceptance rates, only one of the two volume changes (ΔV^{I} or ΔV^{II}) is attempted in any given Monte Carlo event. Equation 3 is not applicable to traditional osmotic simulations because of the pressure difference (the osmotic pressure) that is required to maintain equilibrium. A variation of the standard Gibbs-ensemble method has been suggested by Panagiotopoulos et al.⁴⁸ for simulating equilibria across a semipermeable membrane. In the method of Panagiotopoulos and co-workers, the osmotic pressure is a specified parameter in the acceptance criteria used in the simulation. In the simulation of a pure solvent coexisting with a polymer-rich phase at low temperature, the pressures in the two phases will be equal; thus, eq 3 applies without modification. We have verified this condition by clamping the simulation cells at the mean volumes observed in our constant-pressure simulations and then continuing the simulations as constant-volume simulations. No statistically significant pressure difference developed between the two cells.⁶⁷ This result is consistent with Staudinger's work in the 1920s that found the osmotic pressures of macromolecules to be negligible.

A series of osmotic Gibbs-ensemble simulations were conducted for polymer chains of length 10–100 beads in equilibrium with pure solvent. The simulations were performed in cycles, where each cycle consisted of N attempted particle displacements ($N = N^{\text{I}} + N^{\text{II}}$ is the total number of particles in both cells), one attempted volume change for each phase, and a predetermined number of trial solvent-particle exchanges. For each attempted exchange, the direction of the exchange was chosen randomly and with equal probability. A random position in the receiving cell was determined and an attempt made to move a randomly chosen solvent particle from the other cell. No bias techniques were employed when attempting to insert a solvent particle. The number of attempted particle interchanges in each cycle was chosen to successfully transfer 2–3% of all solvent particles per cycle. This required between 20 and 1000 interchange attempts, depending on the thermodynamic state. In the displacement sequence, the maximum displacement was adjusted to give an average acceptance ratio of about 0.33. The maximum change in the cell volume was adjusted to give an acceptance ratio of about 0.5. The mixtures were equilibrated for 1×10^6 cycles followed by 1×10^6 – 5×10^6 production cycles from which block averages were taken.

The nonbonded potential was truncated at a suitable fraction of the fluctuating simulation box length (generally about $2.5\sigma_{\text{ss}}$). Long-range corrections were added to all calculated thermodynamic quantities assuming that the bead–bead radial distribution functions are unity at larger separations. Periodic boundary conditions were assumed in all three directions.

Tables 1 and 2 present typical results from the osmotic Gibbs-ensemble simulations at imposed pressures $P^* = P\sigma_{\text{ss}}^3/\epsilon_{\text{ss}} = 1.0$ and $P^* = 0.30$ for chain lengths of 20 beads. The uncertainties given in paren-

Table 1. Results of Phase Coexistence Properties of Polymer–Solvent Mixtures from Osmotic Gibbs-Ensemble Simulations for 20-Bead Chains in Monomeric Solvent at $P^* = 1.0^a$

T^*	ϕ	P^*		ρ^*		μ^* (solvent)	
		I	II	I	II	I	II
0.5	0.995(3)	0.991(4)	0.987(4)	0.941(2)	1.026(5)	−3.012	−3.006
0.7	0.996(4)	0.982(5)	0.997(8)	0.897(4)	0.994(2)	−2.996	−2.983
0.9	0.991(5)	0.995(4)	0.989(5)	0.833(7)	0.954(1)	−2.686	−2.609
1.0	0.986(4)	1.004(3)	1.004(8)	0.800(5)	0.935(5)	−2.429	−2.419
1.1	0.979(7)	1.006(3)	1.008(9)	0.768(3)	0.915(3)	−2.390	−2.342
1.2	0.961(1)	0.998(5)	0.989(8)	0.735(2)	0.891(4)	−2.242	−2.249
1.3	0.956(3)	1.003(4)	1.000(7)	0.702(8)	0.872(2)	−2.146	−2.166
1.4	0.936(8)	1.002(6)	1.011(7)	0.670(4)	0.851(3)	−2.085	−2.075
1.5	0.921(4)	1.006(5)	1.017(8)	0.636(5)	0.827(4)	−2.033	−2.044
1.6	0.902(7)	0.999(3)	0.992(9)	0.605(4)	0.806(2)	−2.029	−2.031
1.7	0.874(3)	1.001(9)	1.023(8)	0.568(6)	0.779(2)	−2.025	−2.027
1.8	0.849(4)	1.027(11)	1.016(5)	0.541(9)	0.751(5)	−1.997	−2.013
1.9	0.833(2)	0.987(9)	0.994(9)	0.508(3)	0.731(4)	−2.022	−2.020

^a I and II designate solvent-rich and polymer-rich phases, respectively. ϕ is the number fraction of polymer in the polymer-rich phase. μ^* is the chemical potential of the solvent determined via the Widom insertion method. $T^* = (kT)/\epsilon_{ss}$ is the reduced temperature, and $\rho^* = \rho(\sigma_{ss})^3$ is the reduced density. Uncertainties determined from block averages are given in parentheses.

Table 2. Results of Phase Coexistence Properties of Polymer–Solvent Mixtures from Osmotic Gibbs-Ensemble Simulations for 20-Bead Chains in Monomeric Solvent at $P^* = 0.30^a$

T^*	ϕ	P^*		ρ^*		μ^* (solvent)	
		I	II	I	II	I	II
0.75	0.997(5)	0.293(5)	0.298(6)	0.858(7)	0.934(5)	−3.610	−3.653
1.00	0.981(2)	0.296(4)	0.296(9)	0.741(3)	0.905(5)	−3.436	−3.321
1.25	0.973(6)	0.295(6)	0.297(8)	0.613(4)	0.847(4)	−3.241	−3.188
1.50	0.951(5)	0.296(6)	0.293(7)	0.413(5)	0.782(6)	−3.298	−3.264
1.75	0.921(3)	0.296(9)	0.307(4)	0.244(6)	0.717(2)	−3.620	−3.615
2.00	0.893(2)	0.300(1)	0.296(5)	0.179(8)	0.656(5)	−4.154	−4.121
2.25	0.857(2)	0.299(2)	0.302(9)	0.147(3)	0.586(7)	−4.777	−4.798
2.50	0.820(5)	0.303(5)	0.301(3)	0.126(5)	0.513(2)	−5.422	−5.431

^a See Table 1 for details.

theses are estimated by dividing each simulation run into 10 blocks (after discarding the equilibration period). The reported uncertainties correspond to one standard deviation of the block averages. The virial pressures in the two cells show good agreement within their calculated uncertainties. Tables 1 and 2 also give the calculated values of the chemical potential in each cell, which were determined by the Widom particle insertion method.⁶⁸ The values of the chemical potential are not required for the osmotic Gibbs-ensemble method but can be used to verify that phase coexistence is indeed established. Because the chemical potentials were obtained from the calculations over the entire production run, no individual uncertainty estimates are available. However, the agreement between the solvent chemical potentials in the coexisting phases is comparable to that observed in other studies.^{48,62,69}

Figure 4 shows the phase diagrams obtained using the osmotic Gibbs-ensemble method at three different pressures for 20-bead chains. Isobars in Figure 4 are shown as a function of the polymer number fraction, ϕ_p . Since the critical pressure of the Lennard-Jones fluid is about $P_c^* = 0.1$,⁷⁰ the lowest isobar ($P^* = 0.080$) corresponds to an ordinary solvent, while for the other isobars the solvent is a supercritical fluid. Consequently, a significant charge of solvent into the polymer-rich phase is observed at $P^* = 1.0$, which is about 10 times the estimated critical pressure of the Lennard-Jones solvent. The observed range of solvent absorption seen here may well span the entire range of interest for many engineering applications. Although the critical solution conditions are not reached in these simulations, it is apparent from the subcritical behavior that as the pressure increases, the critical solution temperature

decreases and the critical number fraction increases. These observations are in qualitative agreement with experimental data for polymer–solvent systems^{71,72} and with the prediction of various approximate theories.^{17–20}

Figure 5 illustrates the behavior of the osmotic Gibbs-ensemble method for one of the systems ($P^* = 1.0$) shown in Figure 4 when it is driven to increasingly higher temperatures. Eventually, the true equilibrium will include substantial amounts of polymer in the solvent-rich phase—behavior that cannot be captured in the osmotic Gibbs-ensemble method. Note that at high enough temperatures the osmotic Gibbs-ensemble simulations predict that the coexistence curve rises almost vertically near $\phi_p = 0.65$. This is only slightly higher than the global concentration of polymer in the simulations and is the result of an uncontrolled dilution of the polymer-rich phase, leaving only a few particles (typically fewer than 20) in the pure-solvent cell. With a box length comparable to σ_{ss} , this cell no longer realistically mimics a macroscopic equilibrium fluid, and thus the equilibrium established is spurious. The temperature at which this behavior is first observed is not necessarily above the critical solution temperature. Under these conditions, the barrier in the solvent chemical potential has diminished, much like the curve shown in Figure 1 for $T^* = 3.0$. At these higher temperatures, small fluctuations can cause the polymer-containing cell to “discover” the solvent-rich side of the curve (a result of the flatness of the $T^* = 3.0$ curve shown in Figure 1). At that point, the solution erroneously attempts to match its chemical potential with the pure solvent by diluting itself. In the absence of an applied osmotic pressure in the Gibbs-ensemble method, the solvent cell will dilute itself to the maximum extent

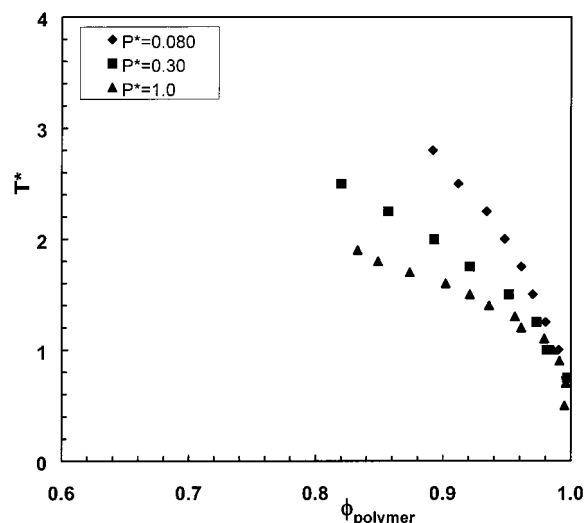


Figure 4. Isobars obtained from osmotic Gibbs-ensemble simulations for 20-bead chains in monomeric solvent at $P^* = 0.080$ (◆), 0.30 (■), and 1.0 (▲).

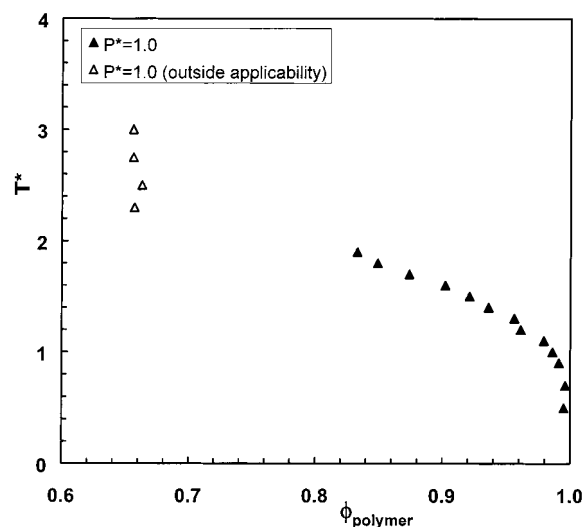


Figure 5. Osmotic Gibbs-ensemble simulation results outside the range of applicability of the method for the $P^* = 1.0$ system shown in Figure 4. The filled symbols (▲) are the same data presented in Figure 4 while the open symbols (△) are simulation results under conditions at which the method is not valid.

possible, given the finite charge of solvent in the two cells. If a simulation with a larger pure-solvent reservoir was attempted, the catastrophic dilution would occur at the same temperature, but the vertical rise would be displaced to the value of ϕ_p that corresponds to the global concentration of polymer in the simulation. The points that are not valid within the low-temperature approximation are shown as open symbols in Figure 5.

The corresponding phase equilibrium calculations for the 20-bead chains at constant temperature are shown in Figure 6. All the results shown are in the regime where the osmotic Gibbs-ensemble method adequately describes the full binary phase equilibrium. Such isotherms are typical of the experimental coexistence studies performed on conventional mixtures of polymer and supercritical solvents.¹³ The reduced slopes of the curves at higher temperatures suggest that the critical pressure decreases and the critical number fraction increases, again in accord with experimental findings. Since $T^*_{\text{critical}} = 1.3$ for the pure Lennard-Jones fluid,⁷⁰

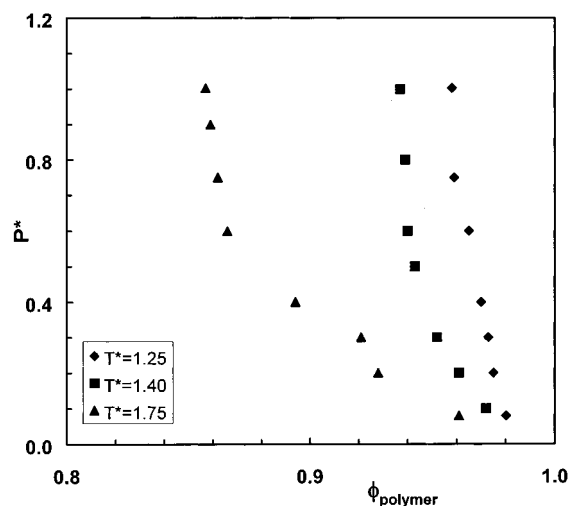


Figure 6. Isotherms obtained from osmotic Gibbs-ensemble simulations for 20-bead chains in monomeric solvent at $T^* = 1.25$ (◆), 1.40 (■), and 1.75 (▲).

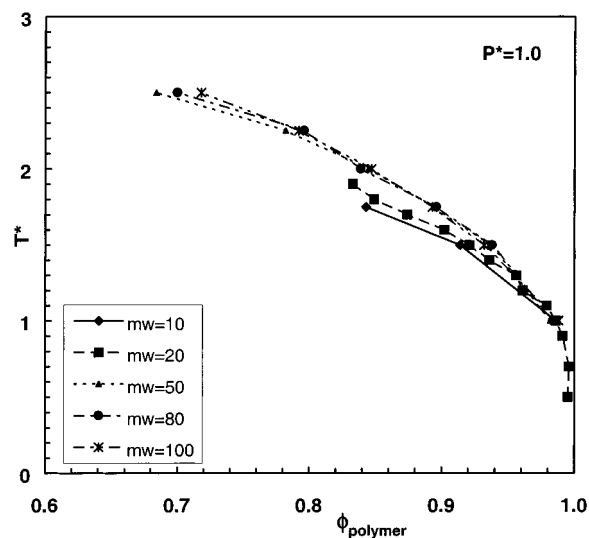


Figure 7. Osmotic Gibbs-ensemble simulation results at $P^* = 1.0$ for chains of length 10 (◆), 20 (■), 50 (▲), 80 (●), and 100 (*). Lines are drawn as a visual guide only.

the results of Figure 6 include both supercritical and subcritical solvent behavior. Note that the simulations were not carried out to low pressures. However, it is apparent that substantial changes in the slope will be required to intersect $\phi_p = 1.0$ at $P^* = 0.0$, again behavior that is consistent with available experimental data.¹³

Figure 7 presents the osmotic Gibbs-ensemble phase diagrams for chains of length 10, 20, 50, 80, and 100 beads at $P^* = 1.0$. All results presented in Figure 7 are within the regime where the osmotic Gibbs-ensemble method adequately describes the full binary phase equilibrium, i.e., the regime where the low-temperature approximation is valid. As expected from approximate theories,^{17–20} the curves are nearly coincident at lower temperatures, and the critical solution temperatures increase with molecular weight. The curves only begin to deviate from one another at higher temperatures—the condition at which the system temperature becomes a reasonably high fraction of its own critical solution temperature. Again, these results are in qualitative agreement with experimental evidence and approximate theories. These findings also indicate that the version

of the Gibbs-ensemble method presented in this study will have a wide range of applicability to studying the phase behavior of polymer solutions containing high molecular weight polymers. The singular behavior exhibited at low temperatures implies that the precise molecular weight employed in the simulation is of little consequence for practical purposes. This finding is important because even with the most advanced configurational bias-sampling techniques, constraints on the length of the polymer chain that can be simulated still exist. The results indicate that relatively short chains can adequately capture the phase behavior of much longer polymers over a substantial range of temperature and pressure.

A final note concerning system size effects. The introduction of periodic boundary conditions greatly suppresses but does not eliminate the effects of a small sample size used in a molecular simulation. Finite-size effects have been demonstrated to be significant for continuous-space systems in two and three dimensions in the Gibbs-ensemble method.⁷³ No such effect for the three-dimensional Lennard-Jones vapor–liquid equilibria has been found. However, it was suggested that this might be a fortuitous cancellation of errors.⁷³ Isolated tests of the effects of the periodic boundary conditions were made for the model used in this work, and no appreciable effect of finite cell sizes was observed.

4. Discussion

The key advantage of the scheme proposed here over currently available techniques is that the method does not require insertions or deletions of chain molecules. Therefore, the method is not limited by the extremely low insertion probability that has thwarted other approaches thus far. The osmotic Gibbs-ensemble method is strikingly efficient at both low temperatures and pressures. Implementation of the method is computationally inexpensive and does not require the use of any new simulation tools or algorithms. The method relies on the assumption that at low temperatures there is virtually no polymer present in the solvent-rich phase. For many engineering applications only the polymer-rich phase of the coexistence curve is of interest anyway; thus, the osmotic Gibbs-ensemble method can readily produce the desired phase envelope—an aspect of polymer solution theory that seems not to have been fully appreciated.

All the results for our simple bead–spring model reported here were obtained using minimal timesaving techniques and no sophisticated sampling methods. Configurational-bias methods^{53,76,77} offer significantly better sampling efficiencies for systems with atomistically detailed potentials. These methods can be incorporated into the osmotic Gibbs-ensemble simulations without adding complexity to the overall scheme. With the addition of bias-sampling algorithms, longer chains and more realistic models for the polymer and solvent could be simulated. Even so, the simple models used here (after suitable adjustments of the energy and size parameters) can be applied to real polymer–solvent systems in the same fashion as traditional coarse-grained polymer theories have been applied.⁶⁷ The advantage of using simulation instead of theory is that the simulation is performed in the continuum (thus is intrinsically compressible) and uses a realistic equation

of state. In addition, any statistical mechanical approximations are minimal, and there is no assumption that the conformations of the chains are composition independent. After fitting the model potential parameters, the long-standing ambiguities concerning the meaning of the individual particles would still exist, but the simulation results could help establish the limitations of the model itself, independent of further theoretical approximations. A preliminary application of this strategy to polymer–supercritical solvent systems will be reported elsewhere.⁷⁸

Acknowledgment. The authors thank Paul Van Tassel for use of his computing resources in the finishing stages of this work. J.K.B. is grateful to the College of Engineering at Wayne State for support through the DeVlieg scholarship.

References and Notes

- (1) Kleintjens, L. A. In *Supercritical Fluids*; Kiran, E., Levelt-Sengers, J. M. H., Eds.; Kluwer Academic: Dordrecht, The Netherlands, 1994.
- (2) Yilgor, I.; McGrath, J. E.; Krukons, V. J. *Polym. Bull. (Berlin)* **1984**, *12*, 491.
- (3) Scholsky, K. M.; O'Conner, K. M.; Weiss, C. S.; Krukons, V. J. *ACS Polym. Prepr.* **1986**, *27*, 140.
- (4) Conaway, J. E.; Graham, J. A.; Rogers, L. B. *J. Chromatogr. Sci.* **1987**, *16*, 102.
- (5) Schmitz, F. P.; Klesper, E. *Polym. Commun.* **1983**, *24*, 142.
- (6) Bowman, L. M.; Meyers, M.; Giddings, J. L. *Sep. Sci. Technol.* **1982**, *17*, 271.
- (7) Mourier, P.; Sassi, P.; Caude, M.; Rosset, R. *Analysis* **1984**, *12*, 229.
- (8) Dhalewadikar, S. V.; McHugh, M. A.; Guckes, T. L. *J. Appl. Polym. Sci.* **1984**, *33*, 521.
- (9) Lele, A. K.; Shine, A. D. *AIChE J.* **1992**, *38*, 742.
- (10) Saus, W. *International Workshop on Supercritical Water & Fluid Chemistry*; Kister, R., Ed.; Springer-Verlag: New York, 1993.
- (11) Matson, D. W.; Fulton, J. L.; Petersen, R. C.; Smith, R. D. *Ind. Eng. Chem. Res.* **1987**, *26*, 2298.
- (12) Sen, Y. L.; Kiran, E. *Proceedings of 2nd International Symposium on Supercritical Fluids*; John Hopkins University: Baltimore, MD, 1991.
- (13) Garg, A.; Gulari, E.; Manke, C. W. *Macromolecules* **1994**, *27*, 5643.
- (14) Garg, A.; Gerhardt, L. J.; Gulari, E.; Manke, C. W. *Proceedings of 2nd International Symposium on Supercritical Fluids*; John Hopkins University: Baltimore, MD, 1991. Gerhardt, L. J.; Garg, A.; Bae, Y.; Manke, C. W.; Gulari, E. *Proceedings of the XIth International Congress of Rheology*; Elsevier: New York, 1992.
- (15) Gerhardt, L. J.; Garg, A.; Manke, C. W.; E. Gulari, E. *J. Polym. Sci., Part B* **1997**, *35*, 523.
- (16) Kiran, E.; Sen, Y. L. In *Supercritical Fluid Engineering Science*; Kiran, E., Brennecke, J. F., Eds.; ACS Symposium Series 514; American Chemical Society: Washington, DC, 1993.
- (17) Flory, P. J. *J. Chem. Phys.* **1941**, *9*, 660; **1942**, *10*, 51.
- (18) Huggins, M. L. *J. Chem. Phys.* **1941**, *9*, 440; *J. Phys. Chem.* **1942**, *46*, 6, 151; *Ann. N.Y. Acad. Sci.* **1942**, *41*, 1.
- (19) Miller, A. R. *Proc. Cambridge Philos. Soc.* **1942**, *38*, 109; **1943**, *39*, 54.
- (20) Guggenheim, E. A. *Proc. R. Soc. London, Ser. A* **1944**, *183*, 203, 213.
- (21) Rosenbluth, M. N.; Rosenbluth, A. W. *J. Chem. Phys.* **1955**, *23*, 356.
- (22) Wall, F. T.; Hiller, L. A.; Wheeler, J. *J. Chem. Phys.* **1954**, *22*, 1036.
- (23) Sariban, A.; Binder, K.; Heermann, D. W. *Phys. Rev. B* **1987**, *35*, 6873. Sariban, A.; Binder, K. *J. Chem. Phys.* **1987**, *86*, 5859.
- (24) Madden, W. G.; Pesci, A. I.; Freed, K. F. *Macromolecules* **1990**, *23*, 1181. Dudowicz, J.; Freed, K. F.; Madden, W. G. *Macromolecules* **1990**, *23*, 4803.
- (25) Madden, W. G. *J. Chem. Phys.* **1990**, *88*, 3934.

- (26) Mackie, A. D.; Panagiotopoulos, A. Z.; Frenkel, D.; Kumar, S. K. *Europhys. Lett.* **1994**, *27*, 549.
- (27) Panagiotopoulos, A. Z.; Wong, V.; Floriano, M. A. *Macromolecules* **1998**, *31*, 912.
- (28) Gromov, D. G.; de Pablo, J. J.; Luna-Barcenas, G.; Sanchez, I. C.; Johnston, K. P. *J. Chem. Phys.* **1998**, *108*, 4647.
- (29) Freed, K. F. *J. Phys. Chem. A* **1985**, *18*, 871. Bawendi, M. G.; Freed, K. F. *J. Chem. Phys.* **1988**, *88*, 2741. Pesci, A. I.; Freed, K. F. *J. Chem. Phys.* **1987**, *87*, 7342. Freed, K. F.; Bawendi, M. G. *J. Phys. Chem.* **1989**, *93*, 2194. Nemirovsky, A. M.; Bawendi, M. G.; Freed, K. F. *J. Chem. Phys.* **1987**, *87*, 7272.
- (30) Lipson, J. E. G. *Macromolecules* **1991**, *24*, 1334; *J. Chem. Phys.* **1992**, *96*, 1418.
- (31) Wertheim, M. S. *J. Chem. Phys.* **1986**, *85*, 2929.
- (32) Wertheim, M. S. *J. Chem. Phys.* **1986**, *87*, 7323.
- (33) Donohue, M. D.; Prausnitz, J. M. *AIChE J.* **1986**, *24*, 849.
- (34) Morris, W. O.; Vimalchand, P.; Donohue, M. D. *Fluid Phase Equilib.* **1987**, *32*, 103.
- (35) Chapman, W. G.; Jackson, G.; Gubbins, K. E. *Mol. Phys.* **1988**, *65*, 1057.
- (36) Chapman, W. G.; Gubbins, K. E.; Jackson, G.; Radosz, M. *Ind. Eng. Chem. Res.* **1990**, *29*, 1709.
- (37) Huang, S. H.; Radosz, M. *Ind. Eng. Chem. Res.* **1990**, *29*, 2284; **1991**, *30*, 1994.
- (38) Schweizer, K. S.; Curro, J. G. *Macromolecules* **1987**, *20*, 1928. Schweizer, K. S.; Curro, J. G. *J. Chem. Phys.* **1989**, *91*, 5059.
- (39) Dickman, R.; Hall, C. K. *J. Chem. Phys.* **1986**, *85*, 3023.
- (40) Honnell, K. G.; Hall, C. K. *J. Chem. Phys.* **1989**, *90*, 1841.
- (41) Chiew, Y. C. *Mol. Phys.* **1989**, *70*, 129.
- (42) Ghonasgi, D.; Chapman, W. G. *J. Chem. Phys.* **1994**, *100*, 6633.
- (43) Chang, J.; Sandler, S. I. *Chem. Eng. Sci.* **1994**, *49*, 2777.
- (44) Taylor, M. P.; Lipson, J. E. G. *J. Chem. Phys.* **1994**, *100*, 518; **1995**, *102*, 2118, 6272.
- (45) Panagiotopoulos, A. Z. *Fluid Phase Equilib.* **1995**, *104*, 185.
- (46) Smit, B. *Fluid Phase Equilib.* **1996**, *116*, 249.
- (47) Panagiotopoulos, A. Z. *Mol. Phys.* **1987**, *61*, 813.
- (48) Panagiotopoulos, A. Z.; Quirke, N.; Stapelton, N. M.; Tildesley, D. J. *Mol. Phys.* **1987**, *63*, 527.
- (49) Meirovitch, H. *Macromolecules* **1985**, *18*, 569.
- (50) Harris, J.; Rice, S. A. *J. Chem. Phys.* **1988**, *88*, 1298.
- (51) Siepman, J. I. *Mol. Phys.* **1987**, *70*, 1145.
- (52) Frenkel, D.; Mooij, G. C. A. M.; Smit, B. *J. Phys.: Condens. Matter* **1992**, *4*, 3053.
- (53) de Pablo, J. J.; Laso, M.; Suter, U. W. *J. Chem. Phys.* **1992**, *96*, 2395.
- (54) Escobedo, F. A.; de Pablo, J. J. *J. Chem. Phys.* **1995**, *103*, 1946.
- (55) Escobedo, F. A.; de Pablo, J. J. *J. Chem. Phys.* **1996**, *105*, 4391.
- (56) Mooij, G. C. A. M.; Frenkel, D.; Smit, B. *J. Phys.: Condens. Matter* **1992**, *4*, L255.
- (57) Siepman, J. I.; Karaborni, S.; Smit, B. *Nature (London)* **1993**, *365*, 330; *J. Am. Chem. Soc.* **1993**, *115*, 6454.
- (58) Smit, B.; Siepman, J. I.; Karaborni, S. *J. Chem. Phys.* **1995**, *102*, 2126.
- (59) de Pablo, J. J.; Laso, M.; Suter, U. W. *J. Chem. Phys.* **1993**, *96*, 6157.
- (60) Laso, M.; de Pablo, J. J.; Suter, U. W. *J. Chem. Phys.* **1992**, *97*, 2817.
- (61) de Pablo, J. J. *Fluid Phase Equilib.* **1995**, *104*, 196.
- (62) Sheng, Y. J.; Panagiotopoulos, A. Z.; Kumar, S. K.; Szeleifer, I. *Macromolecules* **1994**, *27*, 400.
- (63) Kofke, D. A.; Glandt, E. D. *Mol. Phys.* **1988**, *64*, 1105.
- (64) Kofke, D. A. *J. Chem. Phys.* **1994**, *98*, 4149.
- (65) Kofke, D. A. *Mol. Phys.* **1994**, *78*, 1331.
- (66) Mehta, M.; Kofke, D. A. *Chem. Eng. Sci.* **1994**, *49*, 2633.
- (67) Brennan, J. K. Doctoral Thesis, Wayne State University, Detroit, MI, 1998.
- (68) Widom, B. *J. Chem. Phys.* **1963**, *39*, 2808.
- (69) Camp, P. J.; Allen, M. P. *Mol. Phys.* **1996**, *88*, 1459.
- (70) Lotfi, A.; Vrabec, J.; Fischer, J. *Mol. Phys.* **1996**, *76*, 1319.
- (71) Dobashi, T.; Nakata, M.; Kaneko, M. *J. Chem. Phys.* **1980**, *72*, 6692.
- (72) Shinozaki, K.; van Tan, T.; Saito, Y.; Nose, T. *Polymer* **1982**, *23*, 728.
- (73) Recht, J. R.; Panagiotopoulos, A. Z. *Mol. Phys.* **1993**, *80*, 843.
- (74) Brennan, J. K.; Madden, W. G. *Mol. Simul.* **1998**, *20*, 137.
- (75) Escobedo, F. A.; de Pablo, J. J. *Fluid Phase Equilib.* **1995**, *104*, 196.
- (76) Escobedo, F. A.; de Pablo, J. J. *J. Chem. Phys.* **1993**, *102*, 2636.
- (77) Frenkel, D.; Mooij, G. C. A. M.; Smit, B. *J. Phys.: Condens. Matter* **1992**, *4*, 3053.
- (78) Brennan, J. K.; Madden, W. G., to be submitted to *J. Chem. Phys.*

MA0112321